Clinical and Experimental Immunology, 2023, **214**, 219–234
https://doi.org/10.1093/cei/uxad081
Advance access publication 27 July 2023
Research Article

Research Article

The CXCL12-CXCR4-NLRP3 axis promotes Schwann cell pyroptosis and sciatic nerve demyelination in rats

Wei Li[1,‡], Jie Liang[1,‡], Shaohua Li[2], Suli Jiang[1], Meiying Song[1], Shuo Xu[1], Luoyang Wang[1], Haining Meng[3], Dongchang Zhai[4], Lei Tang[4], Yanyan Yang[1] and Bei Zhang[1,*]

[1]Department of Immunology, Medical College of Qingdao University, Qingdao, Shandong Province, China
[2]Department of Laboratory Medicine, The Third People's Hospital of Qingdao, Qingdao, Shandong Province, China
[3]School of Emergency Medicine, Medical College of Qingdao University, Qingdao, Shandong Province, China
[4]Department of Special Medicine, School of Basic Medical College, Qingdao University, Qingdao, Shandong Province, China

[*]Correspondence: Bei Zhang, Department of Immunology, Medical College of Qingdao University, No. 308 Ningxia Road, Qingdao, Shandong, China. Email: zhangbei124@aliyun.com
[‡]Contributed equally.

Abstract

Studies have shown that the activation of the NOD-like receptor protein 3 (NLRP3) inflammasome is detrimental to the functional recovery of the sciatic nerve, but the regulatory mechanisms of the NLRP3 inflammasome in peripheral nerves are unclear. C-X-C motif chemokine 12 (CXCL12) can bind to C-X-C chemokine receptor type 4 (CXCR4) and participate in a wide range of nerve inflammation by regulating the NLRP3 inflammasome. Based on these, we explore whether CXCL12-CXCR4 axis regulates the NLRP3 inflammasome in the peripheral nerve. We found that CXCR4/CXCL12, NLRP3 inflammasome-related components, pyroptosis-related proteins and inflammatory factors in the sciatic nerve injured rats were markedly increased compared with the sham-operated group. AMD3100, a CXCR4 antagonist, reverses the activation of NLRP3 inflammasome, Schwann cell pyroptosis and sciatic nerve demyelination. We further treated rat Schwann cells with LPS (lipopolysaccharide) and adenosine triphosphate (ATP) to mimic the cellular inflammation model of sciatic nerve injury, and the results were consistent with those *in vivo*. In addition, both *in vivo* and *in vitro* experiments demonstrated that AMD3100 treatment reduced the phosphorylation of nuclear factor κB (NF-κB) and the expression of thioredoxin interacting protein (TXNIP), which contributes to activating NLRP3 inflammasome. Therefore, our findings suggest that, after sciatic nerve injury, CXCL12-CXCR4 axis may promote Schwann cell pyroptosis and sciatic nerve demyelination through activating NLRP3 inflammasome and slow the recovery process of the sciatic nerve.

Received 17 April 2023; Revised 6 June 2023; Accepted for publication 26 July 2023

Graphical Abstract

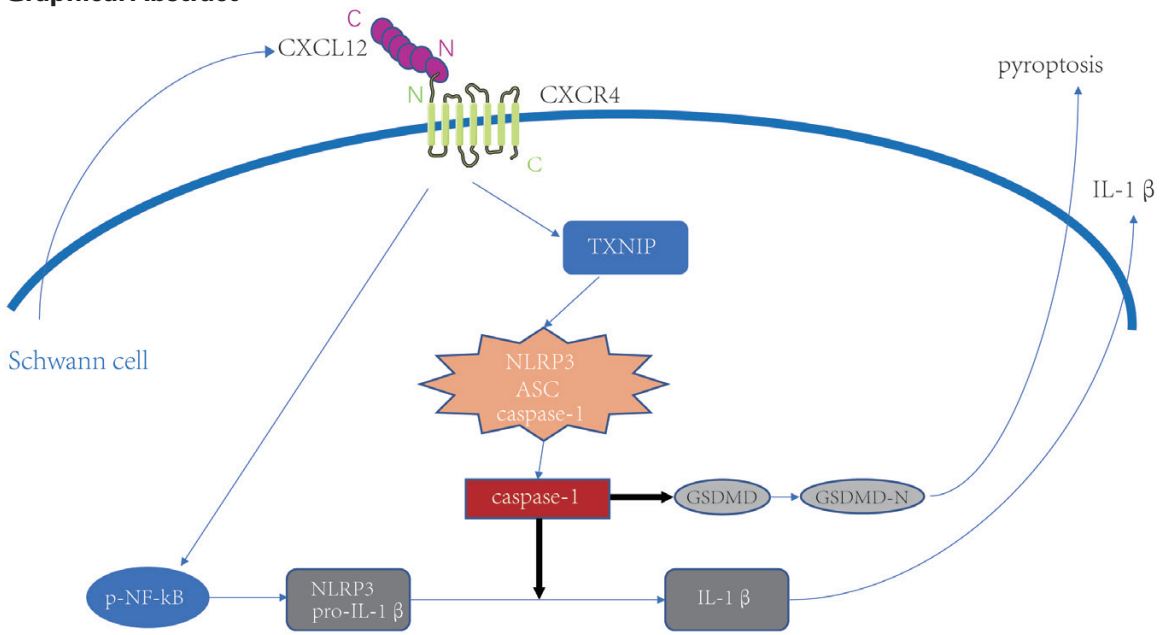

Keywords: sciatic nerve injury, Schwann cell, CXCL12-CXCR4, NLRP3 inflammasome, pyroptosis

Abbreviations: AMD3100: plerixafor, a CXCR4 antagonist; ASC: apoptosis-associated speck-like protein; ATP: adenosine triphosphate; BCA: bicinchoninic acid; BDNF: brain-derived neurotrophic factor; BSA: bovine serum albumin; CCK8: cell counting Kit-8; CXCL12: C-X-C motif chemokine 12; CXCR4: C-X-C chemokine receptor type 4; DAMP: damage-associated molecular pattern; HE: Hematoxylin and eosin; GSDMD: Gasdermin-D; IL-1β: interleukin-1beta; LFB: Luxol Fast Blue; LPS: lipopolysaccharide; MCP-1: monocyte chemoattractant protein-1; NF-κB: nuclear factor κB; NGF: nerve growth factor; NLRP3: NOD-like receptor protein 3; PAGE: sodium dodecyl sulfate polyacrylamide gel electrophoresis; PAMP: pathogen-associated molecular pattern; PBS: phosphate buffered saline; p-NF-κB: the phosphorylation of NF-κB; PVDF: polyvinylidene fluoride; RIPA: radio-immunoprecipitation assay; SD: Sprague Dawley; SDF-1: stromal cell-derived factor 1; SDS-qPCR: quantitative polymerase chain reaction; SFI: Sciatic Nerve Function Index; TNF-α: tumour necrosis factor alpha; TXNIP: thioredoxin interacting protein.

Introduction

The cell bodies of peripheral motor neurons are located in the ventral spinal cord and brainstem, and their long axons wrapped in Schwann cells extend to distant targets such as innervated muscles and organs [1–4]. Therefore, the peripheral nerve axons are easily damaged by various factors such as work-related injuries and traffic accidents. Interestingly, compared with the central nerve, peripheral nerve axons have the ability to partially regenerate and repair after injuries. Schwann cells, which wrap around axons to form myelin sheath, play a key role in the inflammation and regeneration of peripheral nerves after injury. Early in an injury caused by a peripheral nerve crush or cut, Schwann cells at the distal end of the injury are reprogrammed into repair Schwann cells. On the one hand, these repair Schwann cells express some inflammation-related cytokines and chemokines, such as tumour necrosis factor alpha (TNF-α), interleukin-1beta (IL-1β), monocyte chemoattractant protein-1 (MCP-1), participating in the innate immune response including myelin clearance. On the other hand, through the secretion of some neurotrophic factors, such as brain-derived neurotrophic factor (BDNF) and nerve growth factor (NGF), promoting axonal growth to the distal end [5]. However, the inflammatory response accompanying peripheral nerve injury is always involved in the repair process of the injured nerve, and excessive and persistent inflammatory response is not conducive to the regeneration and repair of peripheral nerve [6]. Studies have shown that Schwann cells first respond to the inflammatory response of peripheral nerve injury, thus playing the role of sentinel immune cells in Wallerian degeneration [7–9].

NLRP3 inflammasomes is a complex composed of NLRP3, caspase-1 and adapter apoptosis-associated speck-like protein (ASC) that plays a role in linking NLRP3 and caspase-1, it can respond to the stimulation of damage-associated molecular pattern (DAMP) or pathogen-associated molecular pattern (PAMP) during infection or tissue damage [10]. The activation of NLRP3 inflammasome leads to pyroptosis and the release of inflammatory factors such as IL-1β, which are involved in the inflammatory response of the central and peripheral nerves [11–13]. Numerous studies have shown that the activation of NLRP3 inflammasome exacerbates brain damage and promotes neurodegeneration [14–16], and furthermore, the Gasdermin-D (GSDMD) cleaved by NLRP3 inflammasome induces pyroptosis of neurons and increases neurological damage in Alzheimer's disease [17]. Moreover, the activation of the NLRP3 inflammasome was also found to promote Schwann cell pyroptosis in peripheral nerve Schwann cells [18]. Activation of NLRP3 inflammasome in tumorous Schwann cells of vestibular schwannoma has been reported to lead to increased hearing loss in patients [19]. Recent findings in sciatic nerve-injured mice showed that the functional recovery in the NLRP3 knockout group was markedly better than that in the nonknockout group [20]. Therefore, studying the regulatory mechanism of NLRP3 inflammasome activation will help to provide solutions for alleviating the harm caused by nerve injury.

CXCR4 is expressed in almost all cell types of the peripheral and central nervous system [21], it is predominantly distributed in neurons, Schwann cells are also found to express significantly CXCR4 [22]. CXCL12, also known as stromal

cell-derived factor 1 (SDF-1), has three isoforms, namely SDF-1α, SDF-1β, and SDF-1γ. It has been proven that the expression of these three isoforms is increased in Schwann cells after peripheral nerve injury, of which SDF-1α has been more prevalent in nerves [23, 24]. As the ligand of CXCR4, CXCL12 participates in multiple functions such as cell proliferation, migration, and inflammation through complex intracellular signaling mechanisms after binding to CXCR4 [25]. Moreover, CXCL12 secreted by Schwann cells participate in nerve repair after sciatic nerve crush by interacting with CXCR4 expressed by axons [24, 26], and the increased expression of CXCL12 early after facial nerve injury also promoted the migration of Schwann cells [27]. These have shown that CXCL12 and axonal CXCR4 are beneficial to peripheral nerve regeneration in terms of cell migration, but there is also a considerable amount of literature that proves the adverse role of CXCL12-CXCR4 in inflammatory response. For example, CXCL12 induces primary astrocyte death after interacting with CXCR4 in an autocrine or paracrine manner [28].

In the inflammation of myocardial infarction, overexpression of CXCR4 was found to activate the nuclear translocation and phosphorylation of NF-κB and promote the activation of NLRP3 inflammasome [29]. Studies have also demonstrated that the phosphorylation of NF-κB (p-NF-κB) in inflammatory responses promotes NLRP3 expression and inflammasome activation [30–32]. Expression of CXCR4, CXCL12, TXNIP, and NLRP3 is markedly elevated in neuropathic pain induced by unilateral sciatic nerve chronic contraction injury, and CXCL12-CXCR4 mediates NLRP3 inflammasome activation and increases mechanical pain [33]. In addition, CXCR4 was also found to promote the expression of TXNIP to activate the NLRP3 inflammasome, which is consistent with another previous study of neuroinflammatory pain [34].

TXNIP is a nonenzymatic oxidant that is ubiquitously expressed in a variety of cells and can endogenously inhibit the activity of thioredoxin, a reactive oxygen species scavenging protein [35], which is associated with stroke, depression, Alzheimer's disease, and spinal cord or brain injury [36–40]. In recent years, TXNIP was found to involved in the activation of the downstream NLRP3 inflammasome and pyroptosis, and has received extensive attention in the research progress of nerve injury and pain [41–43]. However, it has not been confirmed whether CXCL12-CXCR4 regulates the NLRP3 inflammasome in Schwann cells after sciatic nerve injury through intermediate signaling molecules such as TXNIP or p-NF-κB, and its effect on sciatic nerve demyelination and neurological recovery have not been demonstrated.

Schwann cells dominates the immune cells within 2 days after peripheral nerve injury, while macrophages, which mainly cleared broken axons and myelin debris, are recruited into the injury site mainly after the second day in the presence of large amounts of chemokines and other cytokines secreted by Schwann cells after the second day [44]. Thus, Schwann cells play an important role as sentinel immune cells following peripheral nerve injury [7, 8]. Therefore, this study takes Schwann cells in the early stage of sciatic nerve injury as the research object to explore the regulatory mechanism of Schwann cells on the inflammatory response after sciatic nerve injury.

Methods and materials

Assessment of RSC96 Schwann cells viability

Cell viability of RSC96 rat Schwann cells (Procell, Cat#CL-0199, RRID: CVCL_4694, Wuhan, China) under different concentrations of LPS (Sigma, Cat# LPS25, Shanghai, China) or AMD3100 (plerixafor) (Selleck, Cat# S3013, Houston, USA) was detected by cell counting Kit-8 (CCK8) (Selleck, Cat# B34302, Houston, USA) assay. Briefly, Schwann cells in good growth state were cultured into a 96-well plate (CELLPRO, Cat# 803096, Jiangsu, China) at 4000 cells per well. After 24 h, the cells were treated with different concentrations of LPS (0, 0.1, 1, 10, and 100 μg/mL) or AMD3100 (1, 2.5, and 5 μg/mL) for additional 24 h. We then disgarded the old serum-containing medium and added 100 μL new serum-free high-glucose DMEM (VivaCell, Cat# C3118-0500, Shanghai, China) and 10 μL of CCK8 reagent to each well. After gentle mixing the plate, cells were incubated for 2 h. Finally, the absorbance of the sample at a wavelength of 450 nm was further analyzed with Synergy Neo2 (BioTek, USA) to reflect the cell viability of Schwann cells.

Detection of RSC96 cell membrane surface proteins

The expression level of CXCR4 on the surface of Schwann cells was detected by flow cytometry. Briefly, 1 μg/mL LPS or 1 mL basal medium was added when the proportion of Schwann cells reaches about 80%, and about 500 000 Schwann cells were collected after 24 h of cell culture. Schwann cells were blocked with blocking buffer (5% bovine serum albumin (BSA, Cat#A8020, Solarbio, Beijing, China) in phosphate buffered saline (PBS, Servicebio, G4202-500ML, Wuhan, China)) for 20 min and were incubated with rabbit anti-CXCR4 antibody (1:100, Absin Cat#abs120406-50μl, Shanghai, China) on ice for 30 min. After washing three times with washing buffer (5% BSA in PBS), Schwann cells were incubated with fluorescein isothiocyanate (FITC)-labeled goat anti-rabbit IgG (1:400, Abcom Cat#ab6717, Cambridge, USA) for 50 minutes at 25°C. After another three times of washing with washing buffer, the expression of CXCR4 on Schwann cell membrane surface were detected with flow cytometer (ACEA Biosciences, California, USA). Flow Jo software was used to analyze the mean fluorescence intensity (MFI), which represents the average expression levels of CXCR4 on the surface of Schwann cell membranes.

Drugs treatment of LPS, ATP, CXCL12, and AMD3100

In the *in vitro* experiments, when the proportion of RSC96 Schwann cells reached about 80%, the new medium (10% fetal bovine serum (FBS, VivaCell, Cat# C04001-500, Shanghai, China), 1% penicillin-streptomycin and 90% high-glucose Dulbecco's Modified Eagle's Medium (DMEM, VivaCell, Cat# C3118-0500, Shanghai, China)) was used to replace the old one, and 2.5 μg/mL AMD3100 (Selleck, Cat# S3013, Houston, USA) was added to the culture flask to preprocess the Schwann cells in the cell incubator (Thermo Fisher, Massachusetts, USA) (37°C, 5%CO_2) for 2 hours. Then, the cells were incubated with 100 ng/ml CXCL12 (Peprotech, Cat#400-32A, New Jersey, USA) and 1 μg/ml LPS (Sigma, Cat# LPS25, Shanghai, China) for 24 h in the cell incubator. Culture medium was further replaced with the fresh serum-free medium (DMEM) without AMD3100, LPS and CXCL12

was replaced, and the 5 mM ATP was added to continue to incubate the cells for 30 minutes in cell incubator. The protein or RNA was then extracted for Western blot or quantitative PCR experiments according to the experimental purposes.

Experimental animals

All the animal experiments in this study adhered to the ARRIVE guidelines 2.0 [45, 46]. We used 8–10 weeks male pathogen-free normal Sprague-Dawley (SD) rats (200–260 g) from Beijing Weitong Lihua Laboratory Animal Technology Corporation (licence No. SCXK (Jing) 2016-0011). Before constructing the sciatic nerve injury model, all rats were housed in Qingdao University Animal Center at room temperature of 22 ± 2°C, a 12 hours light/dark cycle and an environmental humidity of 60%, and given standard laboratory feed and water. Rats were acclimated for 1 week before the experiment. After constructing the sciatic nerve injury model, each rat was placed in a cage alone. Clean bedding was changed for each cage in advance, and some feed and water were placed around the mouth of the rat to facilitate the rat to eat food when they could not easily move around after sciatic nerve injury. All the experimental animal procedures were approved by the Ethics Committee of Qingdao University Medical College. This license complies with the Regulations on Laboratory Animals formulated by the National Science and Technology Commission of China.

Rats were randomly divided into different groups according to the purpose of *in vivo* experiments. The rat sciatic nerve injury model was constructed by the modified sciatic nerve injury method [7, 47]. The rats were anesthetized with sodium pentobarbital (Jisskang, Cat#EI2097, Qingdao, China) (40 mg/kg) intraperitoneally. The sciatic nerve trunk was exposed. In the sciatic nerve injury group and AMD3100 group, the sciatic nerve was vertically clamped with hemostatic forceps for 1 minute, while in the control group, the sciatic nerve was only picked up with the hemostatic forceps and expose for 1 minute without clamp injury. We then carefully repositioned the nerve, irrigated the wound with saline, and finally sutured the wound. AMD3100 group was given 5 mg/kg AMD3100 (Selleck, Cat# S3013, Houston, USA) intraperitoneally 6 hours before surgery. Meanwhile, the control group and sciatic nerve injury group were given equal volumes of normal saline.

Immunofluorescent assay in sciatic nerve Schwann cells

Before sciatic nerve injury, the rats were anesthetized with sodium pentobarbital (Jisskang, Cat#EI2097, Qingdao, China) (40 mg/kg) intraperitoneally. Animals were then euthanized by intraperitoneal injection of 150–200 mg/kg sodium pentobarbital 24 hours after sciatic nerve injury. Sciatic nerve tissues were harvested, fixed with 4% paraformaldehyde for 24 hours, and longitudinally sectioned for dual immunofluorescent staining as previously described [20, 47]. The specific primary antibodies adopted in this experiment are anti-S100B (rabbit, 1:500, Servicebio, Cat# GB11359, Wuhan, China), anti-CXCL12 (mouse, 1:100, Santa Cruz, Cat# ER1902-35, Dallas, USA) and anti-CXCR4 (mouse, 1:500, Santa, Cruz Cat# ER1802-28, Dallas, USA) antibodies, and the secondary antibody are Cy3-labeled goat anti-rabbit IgG (1:200, Abcom, Cat# ab6939, Cambridge, UK) and FITC-labelled goat anti-mouse IgG (1:100, Absin, Cat# ABS20012, Shanghai, China). Finally, images were obtained by Ni-U fluorescence microscopy (Nikon, Japan) after nuclear staining with 4′,6-diamidino-2-phenylindole (DAPI).

Hematoxylin and eosin (HE) and Luxol Fast Blue (LFB) staining

Each animal was euthanized after 24 hours of the sciatic nerve injury. The 1 cm-long sciatic nerve tissues obtained from different groups were fixed, dehydrated, encapsulated in paraffin, and dissected vertically into slices with a thickness of 4 μm and a length of 1 cm. The tissue sections were stained according to the standard procedure of HE staining to observe the infiltration of inflammatory cells. LFB staining was used to stain and observe the demyelination of distal nerve injury in different groups.

Western blot analysis

After the nerve tissues were taken out, proteins were extracted immediately or stored temporarily in a refrigerator at −80°C until proteins were extracted the next day. The proteins of tissues or Schwann cells were extracted on ice with radio-immunoprecipitation assay (RIPA) lysis buffer (CWBIO, Cat# CW2333S, Jiangsu, China) mixed with protease inhibitors (TOPSCIENCE, Cat# C0001, Shanghai, China) and phosphatase inhibitors (TOPSCIENCE, Cat# C0002 and C0003, Shanghai, China). The total protein concentration was determined by a bicinchoninic acid (BCA) Protein Assay Kit (CWBIO, Cat# CW0014S, Jiangsu, China). Next, sodium dodecyl sulfate polyacrylamide gel electrophoresis (SDS-PAGE) buffer (CWBIO, Cat# CW0028S, Jiangsu, China) was used for protein denaturation (10 min at 99°C). Then the protein lysates were separated by SDS-PAGE gels and then transferred to polyvinylidene fluoride (PVDF) membranes (Sigma, Cat# 03010040001, Shanghai, China). The PVDF membranes were blocked with 5% skim milk powder (Phygene, Cat# PH1519, Zhou Fu, China) in TBST (Tris–buffered saline with 0.1% Tween 20) at about 25°C for 1 hour. After washing three times with TBST, the PVDF membranes were incubated with the following primary antibodies at 4°C overnight: rabbit anti-NLRP3 antibody (1:1000, Abcom, Cat#ab263899, Cambridge, UK), rabbit anti-ASC antibody (1:1000, Bioss, Cat#bs-6741R, Beijing, China), rabbit anti-caspase-1 antibody (1:1000, Bioss, Cat#bs-0169R, Beijing, China), rabbit anti-IL-1β antibody (1:1000, Bioss, Cat#bs-0812R, Beijing, China), rabbit anti-p-NF-κB antibody (1:1000, Bioss, Cat#bs-3543R, Beijing, China), mouse anti-GSDMD antibody (1:500, Santa Cruz, Dallas, USA), mouse anti-TXNIP antibody (1:500, Santa Cruz, Dallas, USA), mouse anti-CXCR4 antibody (1:500, Santa Cruz, Dallas, USA), rabbit anti-CXCL12 antibody (1:1000, Abcom, Cat#ab25117, Cambridge, UK), rabbit anti-β-actin antibody (1:20 000, Abways Cat# AB0035, Shanghai, China) and rabbit anti-GAPDH antibody (1:5000, Beyotime, Cat# AF1186, Shanghai, China). The PVDF membranes was then washed with TBST three times and were incubated with the horseradish peroxidase (HRP)-conjugated anti-rabbit or anti-mouse IgG secondary antibody (1:10 000, Absin, Cat# LS-C707606-100, Shanghai, China) at room temperature for 2 h. Thereafter, PVDF membranes were washed with TBST for another three times and detected with Affinity ECL kit (picogram) (Affinity, Cat# KF8001, Jiangsu, China) and visualized by an imager (Amersham Imager 680, Japan). Finally,

the densities of these protein were analyzed with ImageJ 1.4.7 software (National Institutes of Health, Bethesda, USA).

Quantitative polymerase chain reaction (qPCR)

Total RNA was isolated from Schwann cells using RNAiso Plus reagent (Takara, Cat# 9108, Dalian, China), and the concentration and integrity were evaluated by using a BioPhotometer (Eppendorf, Hamburg, Germany). The mRNA was then reverse transcribed into complementary DNA (cDNA) which was subsequently amplified by PCR with following specific primers: CXCL12, forward *5′-CGC TCT GCA TCA GTG ACG GTA AG-3′* and reverse *5′-CGT TGG CTC TGG CGA CAT GG-3′*; NLRP3, forward *5′-GAG CTG GAC CTC AGT GAC AAT GC-3′* and reverse *5′-ACC AAT GCG AGA TCC TGA CAA CAC-3′*; ASC, forward *5′-GAA GTG GAC GGA GTG CTG GAT G-3′* and reverse *5′-CTT GTC TTG GCT GGT GGT CTC TG-3′*. The expression of the mRNA was quantified by RT-qPCR using the CFX96 real-time PCR detection system (Bio-Rad, California, USA). The relative expression levels of target genes were equal to $2^{-\Delta\Delta CT}$ calculated by the cycle threshold (CT) method [48, 49].

Sciatic nerve function index (SFI)

The SFI is an invasive and commonly used research method that reflect the recovery of sciatic nerve function after sciatic nerve injury through measuring the footprints of mice and rats [47, 50–52]. We measured SFI of rats on days 1, 4, 8, 12, 16, 20, and 24 after sciatic nerve injury. Specifically, rat feet on the operative and contralateral sides were stained with ink. Then we let them walk freely from the beginning to the end in the camera obscura, leaving the footprints on the white paper. We label the operative side footprint as E, and the contralateral footprint as N. Three variables were measured on both sides: footprint length (PL), toe spread (TS), and intermediary toe spread (IT). The calculating formula of SFI is – 38.3(EPL – NPL)/NPL + 109.5(ETS – NTS)/NTS + 13.3(EIT – NIT)/NIT – 8.8. The SFI score of rats vary from –100 to 0. The closer the SFI score is to –100, the greater the loss of sciatic nerve function.

Statistical analysis

The data were analyzed by GraphPad Prism 7.0.0 (GraphPad Software, California, USA) and are presented as mean ± SD. Two-way analysis of variance (ANOVA) or Student's t test was used for statistical analysis according to different groups. $P < 0.05$ was considered significant in the results.

Results

Inflammatory Schwann cells increases NLRP3 inflammasome activation and synchronously express CXCL12 and CXCR4

RSC96 rat Schwann cells treated by LPS were used *in vitro* to simulate the injured Schwann cell inflammation model *in vivo*. First, to determine the appropriate concentration of LPS as an inducer of Schwann cell inflammation model, we first performed CCK8 to test the effect of different concentrations of LPS (0, 0.1, 1, 10, and 100 μg/mL) on Schwann cell activity, and then screened out the appropriate concentration of LPS by quantitative PCR detecting several key molecules (NLRP3, ASC, CXCL12) during the experiments. The results showed that cell viability was decreased only at 100 μg/mL LPS after 24 hours treatment, while the other concentrations had no significant effect on RSC96 cells (Figure 1A). Therefore, the concentration of LPS below 10 μg/mL is appropriate in the subsequent experiments. Then qPCR demonstrated that both 1 and 10 μg/mL of LPS could up-regulate the expression of CXCL12 and NLRP3 inflammasome-related components (Figure 1B). So, we finally adopted 1 μg/mL LPS to stimulate RSC96 cells for 6 and 24 hours, respectively. Western blot results showed that compared with the control group, the NLRP3 inflammasome in the LPS treatment group for 6 hours was not activated, while the NLRP3 inflammasome was activated after 24 hours of LPS stimulation, and more inflammatory factor IL-1β was produced (Figure 1C).

Consistent with NLRP3 inflammasome activation, CXCR4 and CXCL12 were also not increased at 6 hours, but increased at 24 hours (Figure 1D). Flow cytometry further showed that compared with 0 hours group, the expression of CXCR4 on the surface of RSC96 cell stimulated with LPS for 24 hours was the most significant (Figure 1E). These results showed that compared with the 0 hours group, NLRP3 inflammasomes of RSC96 Schwann cells were activated after stimulated with 1 μg/mL LPS for 24 hours *in vitro*, and the expressions of CXCL12 and CXCR4 were up-regulated at the same time.

CXCL12-CXCR4 promotes the activation of NLRP3 inflammasome and inflammatory response in RSC96 cells

AMD3100 is a highly specific and effective inhibitor that blocking CXCR4 signal transduction, and has been widely used in the studies of CXCR4 signaling pathways [53]. We first detected the effect of AMD3100 on the viability of RSC96 cells using CCK-8 and found that AMD3100 had no statistically different effect (1, 2.5, and 5 μg/ml AMD3100 for 24 hours) on the viability of RSC96 cells compared with 0 μg/ml AMD3100 (Figure 2A). Here, we use 2.5 μg/ml of AMD3100 to inhibit the interaction between CXCL12 and CXCR4. The results showed that AMD3100 significantly reduced the expression of CXCR4 and the protein levels of NLRP3 inflammasome-associated components (NLRP3, ASC, and caspase-1) compared with LPS + ATP and LPS + ATP + CXCL12 groups (Figure 2B and C). However, there was no statistical difference between the LPS + ATP + CXCL12 group and the LPS + ATP group, indicating that exogenous CXCL12 did not further promote the inflammatory response of Schwann cells.

The above results may be due to the fact that cells in the LPS + ATP inflammatory model group secrete enough CXCL12 to combine with CXCR4 on the cell surface to play a pro-inflammatory role. In order to directly prove that Schwann cells can produce CXCL12 and interact with CXCR4 on the cell membrane in an autocrine or paracrine manner to promote the activation of NLRP3 inflammasome, we further detected NLRP3, caspase-1, and IL-1β by western blot experiment without exogenous CXCL12 (Figure 3). The results proved our hypothesis above that Schwann cells can indeed produce enough CXCL12 after LPS treatment, combine with CXCR4 on the cell membrane, and promote the activation of NLRP3 inflammasome. Therefore, exogenous treatment with CXCL12 did not further increase the inflammatory response of Schwann cells. Together, the results suggest that CXCL12 produced by Schwann cells can bind to CXCR4 in an autocrine manner to promote intracellular NLRP3 inflammasome activation.

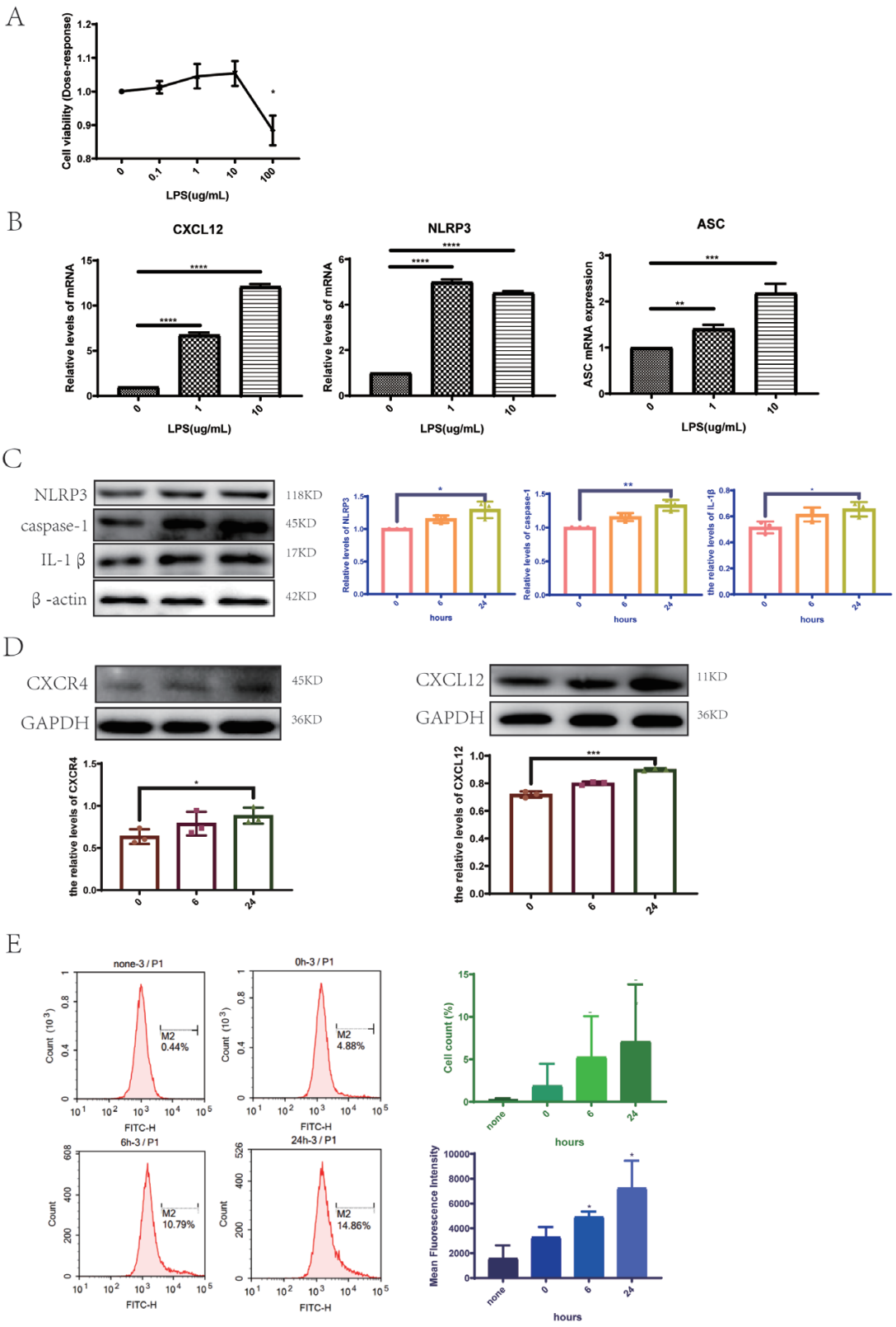

Figure 1. LPS promotes the activation of NLRP3 inflammasome and the expression of CXCR4 and CXCL12 in RSC96 Schwann cells. (A) CCK-8 was used to analyze the effect of different concentrations of LPS on the viability of RSC96 cells. (B) The mRNA levels of NLRP3, ASC, and CXCL12 after LPS (0, 1, 10 μg/mL) treatment. (C) The protein levels of NLRP3 inflammasome components and downstream inflammatory factors were increased in Schwann cells treated with 1 μg/mL LPS for 24 hours. (D) The protein levels of CXCR4 and CXCL12 were up-regulated in Schwann cells treated with 1 μg/mL LPS for 24 hours. (E) The percentage and mean fluorescence intensity of CXCR4 positive cells in different treatment groups were detected by flow cytometry. None (blank group): the group was treated without LPS and CXCR4 antibodies; 0 h: the group was treated with LPS stimulation for 0 hours; 6 h: the group was treated with LPS stimulation for 6 hours; 24 h: the group was treated with LPS stimulation for 24 hours. The expression of CXCR4 on Schwann cell membrane surface was also obvious after 24 hours of LPS treatment. Data are expressed as the mean ± SD of three independent experiments. *$P < 0.05$, **$P < 0.01$, ***$P < 0.001$, ****$P < 0.0001$ (Student's *t* test).

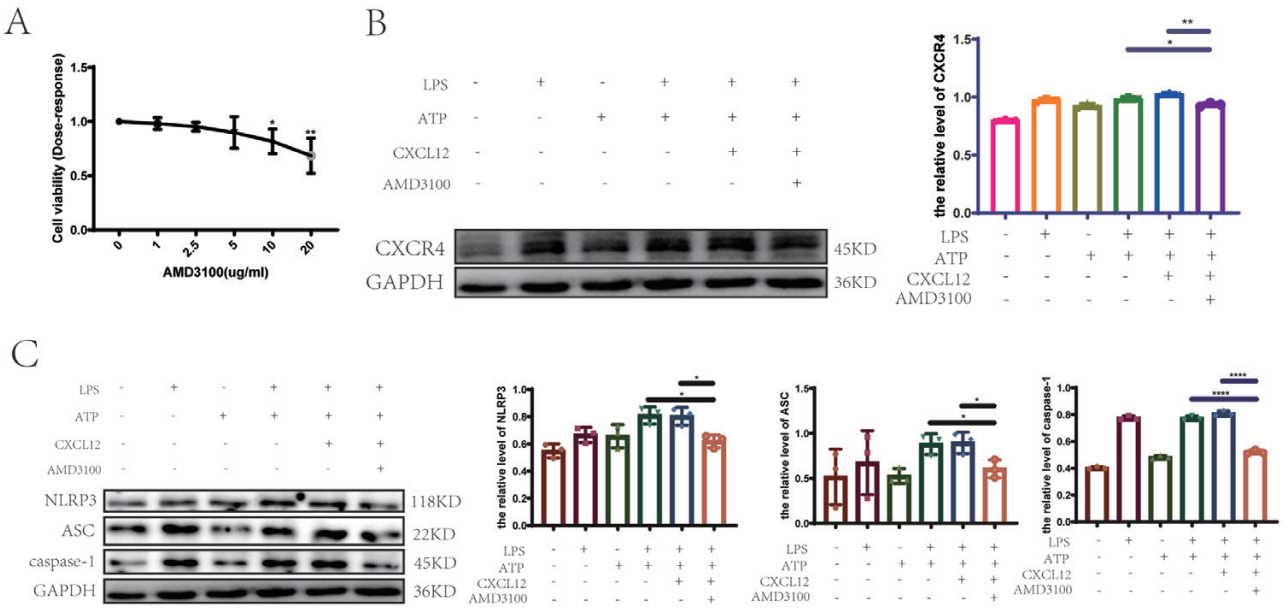

Figure 2. The effects of exogenous CXCL12 and AMD3100 on the expression of CXCR4 and the activation of NLRP3 inflammasome in RSC96 Schwann cells. (A) CCK-8 assay was used to detect the effect of different concentrations of AMD3100 on cell viability of Schwann cells. (B) CXCL12 treatment did not markedly promote the expression of CXCR4 compared with LPS + ATP group, but AMD3100 (2.5 μg/mL) markedly reduced the expression of CXCR4 compared with both LPS + ATP and LPS + ATP + CXCL12 groups. (C) CXCL12 treatment did not markedly increase the protein of NLRP3, ASC and caspase-1 which represent the activation of NLRP3 inflammasome compared with LPS + ATP group, but NLRP3, ASC and caspase-1 were markedly reduced compared with both LPS + ATP group and LPS + ATP + CXCL12 group after the treatment of AMD3100 (2.5 μg/mL). Data are expressed as the mean ± SD of three independent experiments. *$P < 0.05$, **$P < 0.01$, ****$P < 0.0001$ (Student's t test).

CXCL12-CXCR4 promotes RSC96 Schwann cells pyroptosis

The activation of NLRP3 inflammasome is an important condition for inducing pyroptosis [54]. Therefore, we further explored whether CXCL12-CXCR4 affects the pyroptosis of Schwann cells. To this end, we treated RSC96 cells with exogenous CXCL12 and AMD3100, respectively for 24 hours. Western blot analysis showed that compared with LPS + ATP group, exogenous CXCL12 treatment did not markedly increase pyroptosis, but AMD3100 treatment markedly reduced the expression of pyroptosis-related proteins GSDMD and IL-1β (Figure 4A). In addition, transmission electron microscopy was use to observe the morphology of Schwann cells membrane rupture and found that the degree of cell membrane rupture of inflammatory Schwann cells in LPS + ATP group was increased and the cytoplasm was more transparent compared with Control group and LPS + ATP + AMD3100 group, indicating that more contents were released out of the membrane. And compared with Control group, the cells in the LPS + ATP + AMD3100 group became more swollen and there were more bubble-like protrusions on the surface of cell membrane (Figure 2B). These indicated that AMD3100 could reduce Schwann cell pyroptosis in LPS + ATP group. Therefore, the above results indicated that CXCL12 can interact with CXCR4 to promote tpyroptosis in RSC96 Schwan cells.

Inflammasome-related components, CXCL12 and CXCR4, are upregulated after sciatic nerve injury

In order to better verify our hypothesis, we have successfully constructed the rat sciatic nerve clamp injury model based on the existing methods [47, 55] (Figure 5A). Sciatic nerve-injury and sham-operated tissues were obtained from rats 6 and 24 hours after injury, respectively. Compared with the sham-operated group, the NLRP3 inflammasome components such as NLRP3 and ASC were markedly expressed in the injured group 24 hours after injury. In addition, NF-κB, an important pro-inflammatory nuclear transcription factor in the inflammatory signal [56], was markedly expressed in the injured group at 24 hours after injury (Figure 5B). These indicated that the inflammatory response was more obvious at 24 hours after sciatic nerve injury, and the NLRP3 inflammasome was obviously activated. In addition, we also found that the expressions of CXCR4 and CXCL12 were upregulated 24 h after sciatic nerve injury compared with the sham-operated group (Figure 5C).

S100B mainly exists in the cytoplasm and nucleus of glial cells and Schwann cells in nervous systems [57], and is often localized by immunofluorescence staining as a marker of Schwann cells [58]. Therefore, we performed immunofluorescence staining using an anti-S100B antibody for. It was found that 24 hours post sciatic nerve injury, Schwann cells expressed higher CXCR4 and CXCL12 in the cytoplasm, and CXCL12 also had a more obvious intercellular distribution (Figure 5D and E), indicating that part of the CXCL12 expressed by Schwann cells was secreted into the extracellular space to play some roles. Together, these results suggest that expression of CXCR4 and CXCL12 is coordinated with inflammatory response in injured tissues and the marked activation of NLRP3 inflammasome.

AMD3100 reduces the inflammatory response after sciatic nerve injury

AMD3100 (5 mg/kg) was intraperitoneally injected into rats 6 hours before the establishment of the sciatic nerve injury model to specifically block the interaction between CXCL12 and CXCR4. AMD3100 markedly reduced the expression

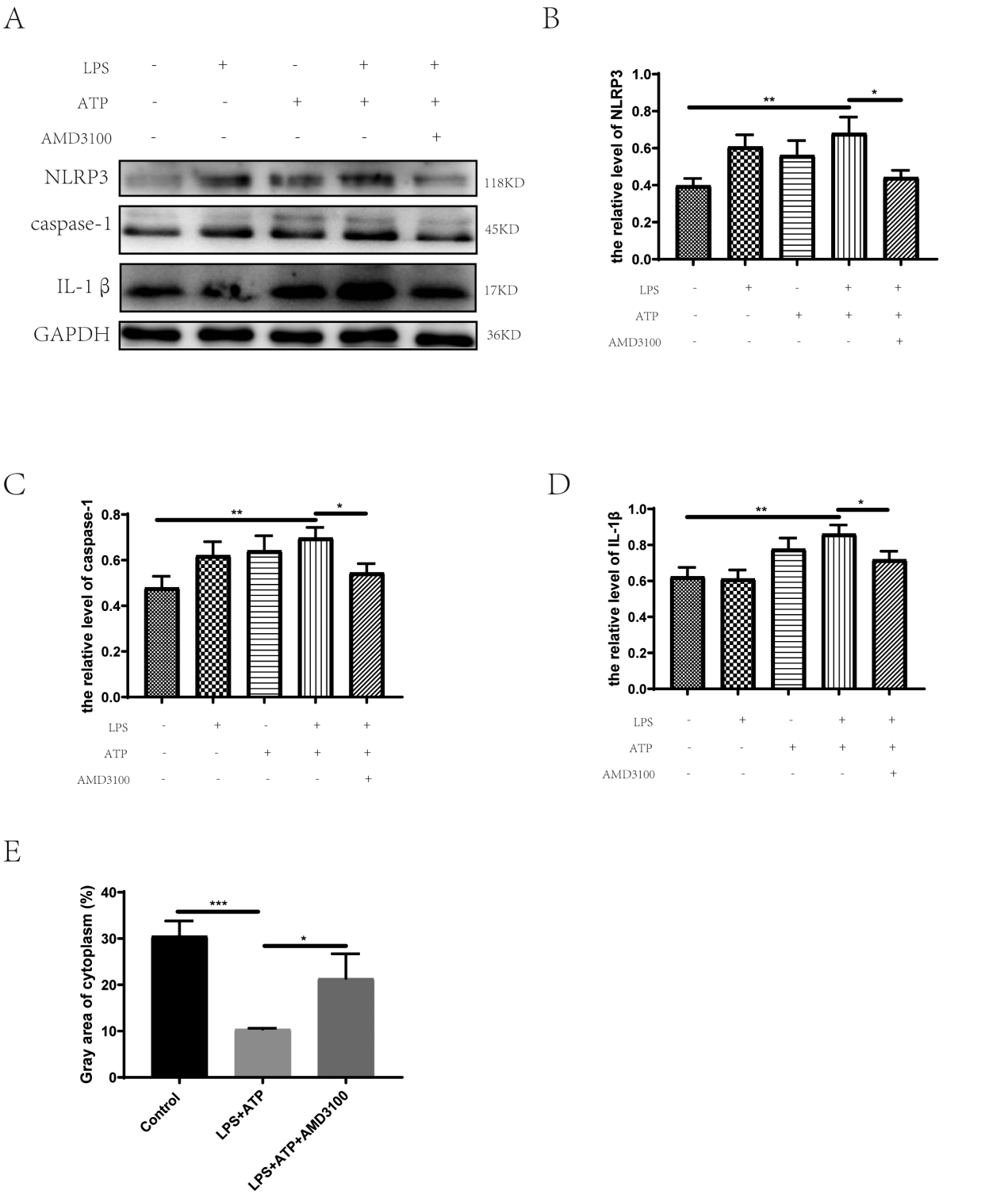

Figure 3. CXCL12 derived from Schwann cells can interact with CXCR4 on the surface of its own cell membrane in an autocrine manner to promote the activation of NLRP3 inflammasome and Schwann cell pyroptosis. (A) Compared with LPS+ + ATP group, AMD3100 attenuates the activation of NLRP3 inflammasome in Schwann cells after blocking CXCL12 and CXCR4. (B–D). The quantitative analysis results showed that AMD3100 attenuates the expression of NLRP3, caspase-1 and IL-1β compared with LPS+ + ATP group. (E) The quantitative analysis results showed that AMD3100 decreases the pyroptosis of Schwann cells compared with LPS+ + ATP group. Data are expressed as the mean ± ± SD of three independent experiments. **P* < < 0.05, ***P* < < 0.01 (Student's *t* test).

of the inflammatory factor IL-1β and reversed the level of NLRP3 24 hours after sciatic nerve injury in rats (Figure 6A). Immunohistochemical results also showed that AMD3100 reduced the expression of NLRP3 in Schwann cells (Figure 6B). In addition, HE staining showed that AMD3100 reduced the infiltration of inflammatory cells (Figure 6C), further suggesting that AMD3100 treatment reduced the inflammatory response after sciatic nerve injury.

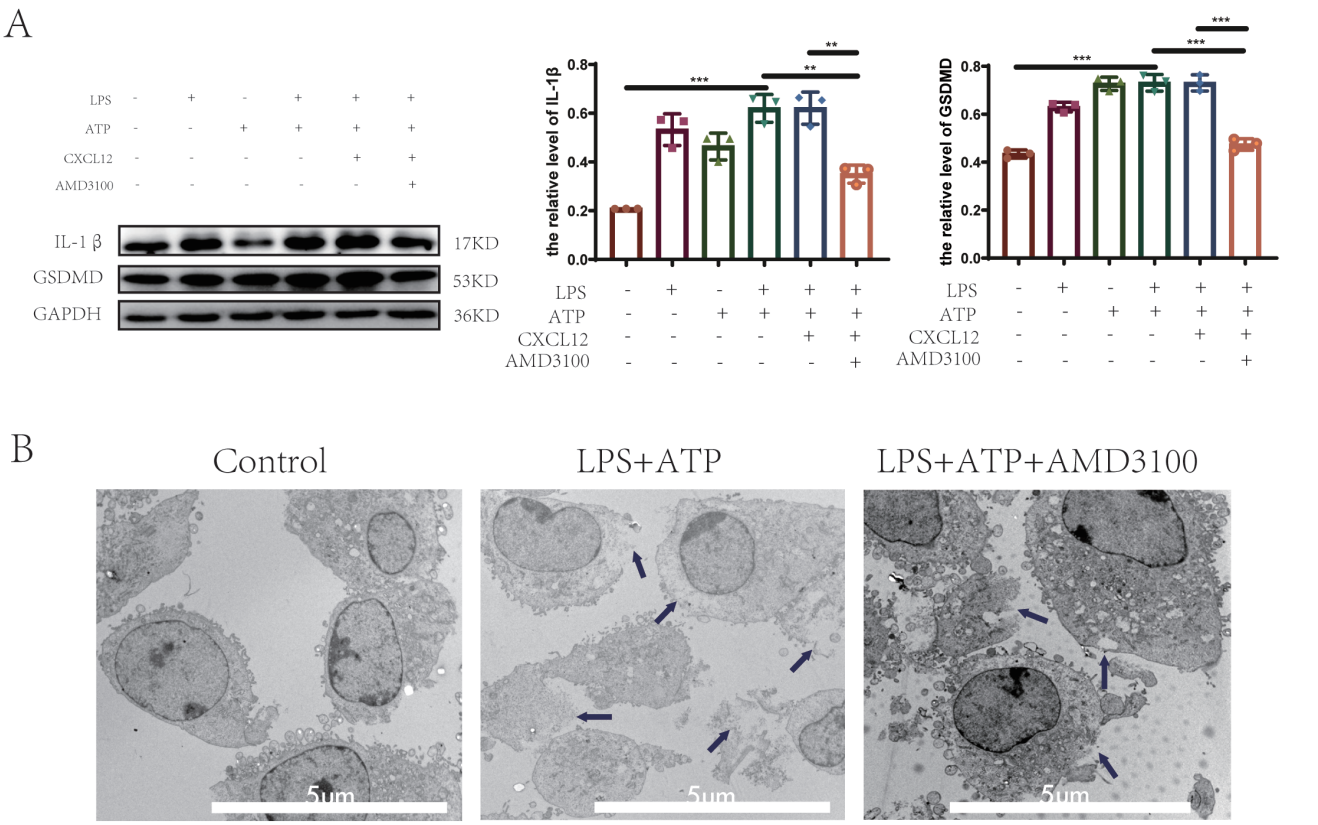

Figure 4. The effects of exogenous CXCL12 and AMD3100 on RSC96 Schwann cell pyroptosis. (A) CXCL12 treatment did not markedly increase the expression of pyroptosis-related proteins GSDMD and IL-1β compared with LPS + ATP group, but that were markedly reduced through AMD3100 (2.5 μg/mL) treatment compared with both LPS + ATP and LPS + ATP + CXCL12 groups. Data are expressed as the mean ± SD of three independent experiments. $^{*}P < 0.05$, $^{**}P < 0.01$, $^{***}P < 0.001$ (Student's *t* test). (B) Comparison of the degree of cell membrane rupture induced by pyroptosis in Control, LPS + ATP and LPS + ATP + AMD3100 groups under transmission electron microscopy. AMD3100 reduced the levels of cell membrane rupture compared with LPS + ATP group. Scale bars: 5 μm.

AMD3100 reduces pyroptosis and sciatic nerve demyelination in rats

GSDMD, as the main marker of pyroptosis, aggregates into pore-like channels on the cell membrane, leading to the decrease of osmotic pressure in cells, and finally the cells burst and die [59]. In addition, caspase-1, the upstream regulating protein of GSDMD, is also a commonly used indicator for detecting pyroptosis [60]. Immunoblotting analysis revealed that AMD3100 treatment notably reduced the expression of GSDMD and caspase-1 in injured tissues (Figure 7A). Next, we used the Schwann cell-specific marker protein S100B [61] to reflect the number of Schwann cells in the sciatic nerve by immunofluorescence. Compared with the sham-operated group, the number of Schwann cells in the distal stump of the injured group was markedly decreased, and AMD3100 treatment reversed the obviously decreased Schwann cells in the injured group, indicating that AMD3100 treatment reduced the death of Schwann cells in the injured sciatic nerve (Figure 7B). In addition, LFB staining was used to observe sciatic nerve demyelination, and it was found that AMD3100 treatment alleviated the demyelination caused by sciatic nerve injury (Figure 7C). The results suggest that AMD3100 may reduce sciatic nerve demyelination by reducing the pyroptosis of Schwann cells in the distal stump of the injured sciatic nerve after blocking the interaction of CXCL12 and CXCR4. Then we used SFI to analyze the recovery of sciatic nerve function over time based on the footprint following sciatic nerve injury. We tracked the footprints of rats on days 1, 4, 8, 12, 16, and 20 after sciatic nerve injury and found that AMD3100 treatment promoted the functional recovery of the sciatic nerve (Figure 7D). In conclusion, these results suggest that AMD3100 may reduce sciatic nerve demyelination and promote functional recovery of sciatic nerve to some extent by reducing pyroptosis of Schwann cells after blocking CXCR4.

CXCL12-CXCR4 may promote the activation of NLRP3 inflammasome through p-NF-κB and TXNIP

TXNIP, as an upstream regulator of the NLRP3 inflammasome, has been found to increase peripheral nerve injury-induced neuropathic pain by promoting the activation of the NLRP3 inflammasome [62]. pNF-κB is a key nuclear transcription factor in the inflammatory response signaling pathway, which promotes the expression of NLRP3 and pro-IL-1β [63]. Previous studies have shown that CXCR4 can promote the nuclear translocation and phosphorylation of NF-κB, enhancing inflammatory response [29, 64]. To verify whether CXCL12-CXCR4 axis plays a proinflammatory role through p-NF-κB and TXNIP in peripheral nerve Schwann cells, western blot experiments were performed. The results showed that the cells in the LPS + ATP group had obvious p-NF-κB and TXNIP expression compared with the control group, and AMD3100 could markedly reduce NF-κBtheir expression in the cells

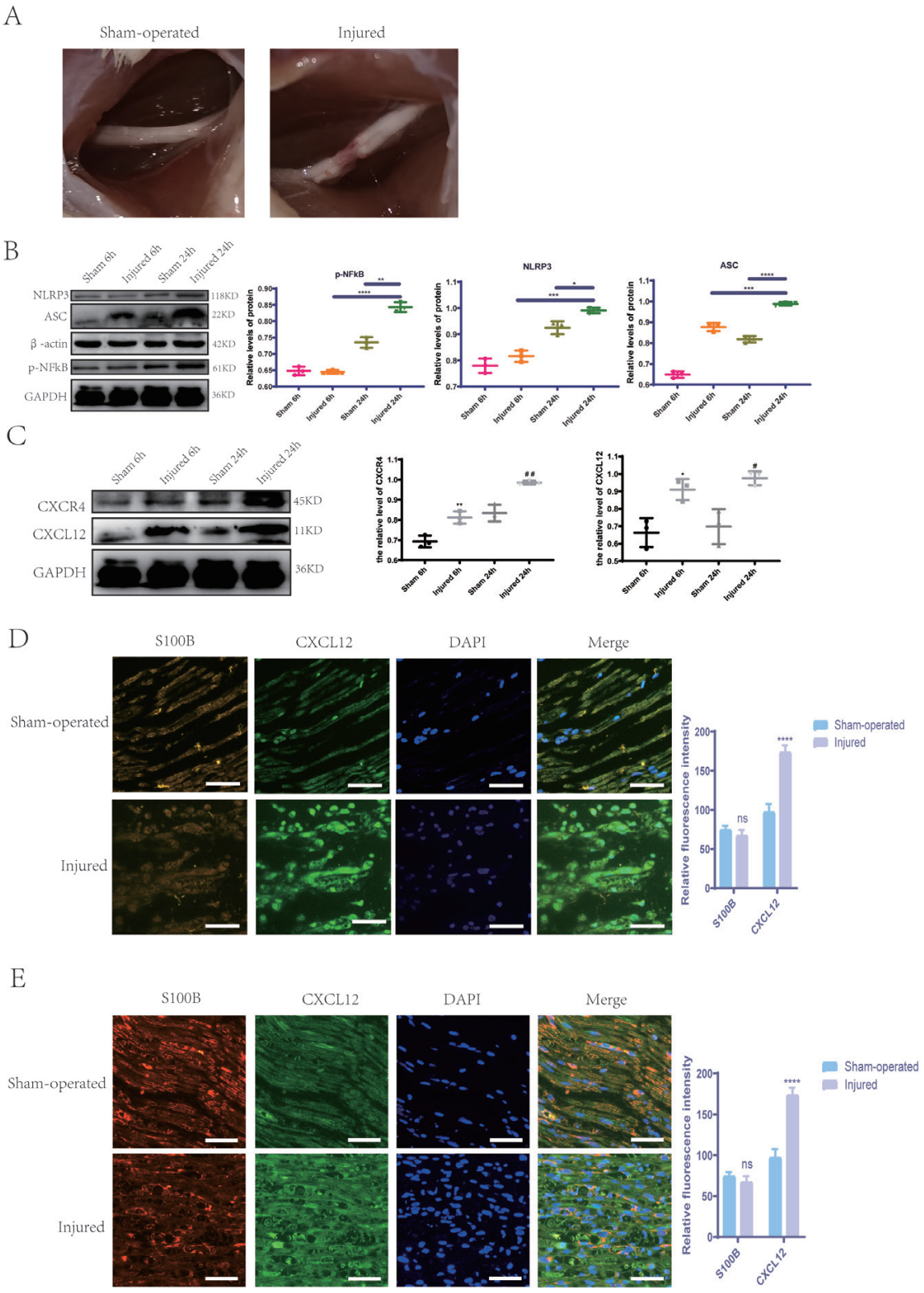

Figure 5. Protein levels of inflammasome-related components, CXCL12 and CXCR4 after sciatic nerve injury in sciatic nerve tissue. (A) Construction of a sciatic nerve clamp injury model. The sham-operated group had no nerve crush injury, while the injured group had nerve crush injury. (B) The protein levels of NLRP3, ASC and p-NF-κB increased significantly at 24 h after sciatic nerve injury compared with the sham group at 24 h and the injured group at 6 h. (C) the expression of CXCR4 and CXCL12 were more obvious than the sham group at 24 h and the injured group at 6 h. (D, E) Immunofluorescence staining of CXCL12 (FITC) (D) and CXCR4 (FITC) (E) in Schwann cells at the distal longitudinal section of sciatic nerve injury site 24 hours after injury. Scale bars: 100 μm. Data are expressed as the mean ± SD of three independent experiments (n = 12 (B, C) and 6 (A, D, E)). $^{*}P < 0.05$, $^{**}P < 0.01$, $^{***}P < 0.001$, $^{****}P < 0.0001$; $^{\#}P < 0.05$, $^{\#\#}P < 0.01$, vs. the sham-operated group in 24 h (C, D, E) (Student's t test).

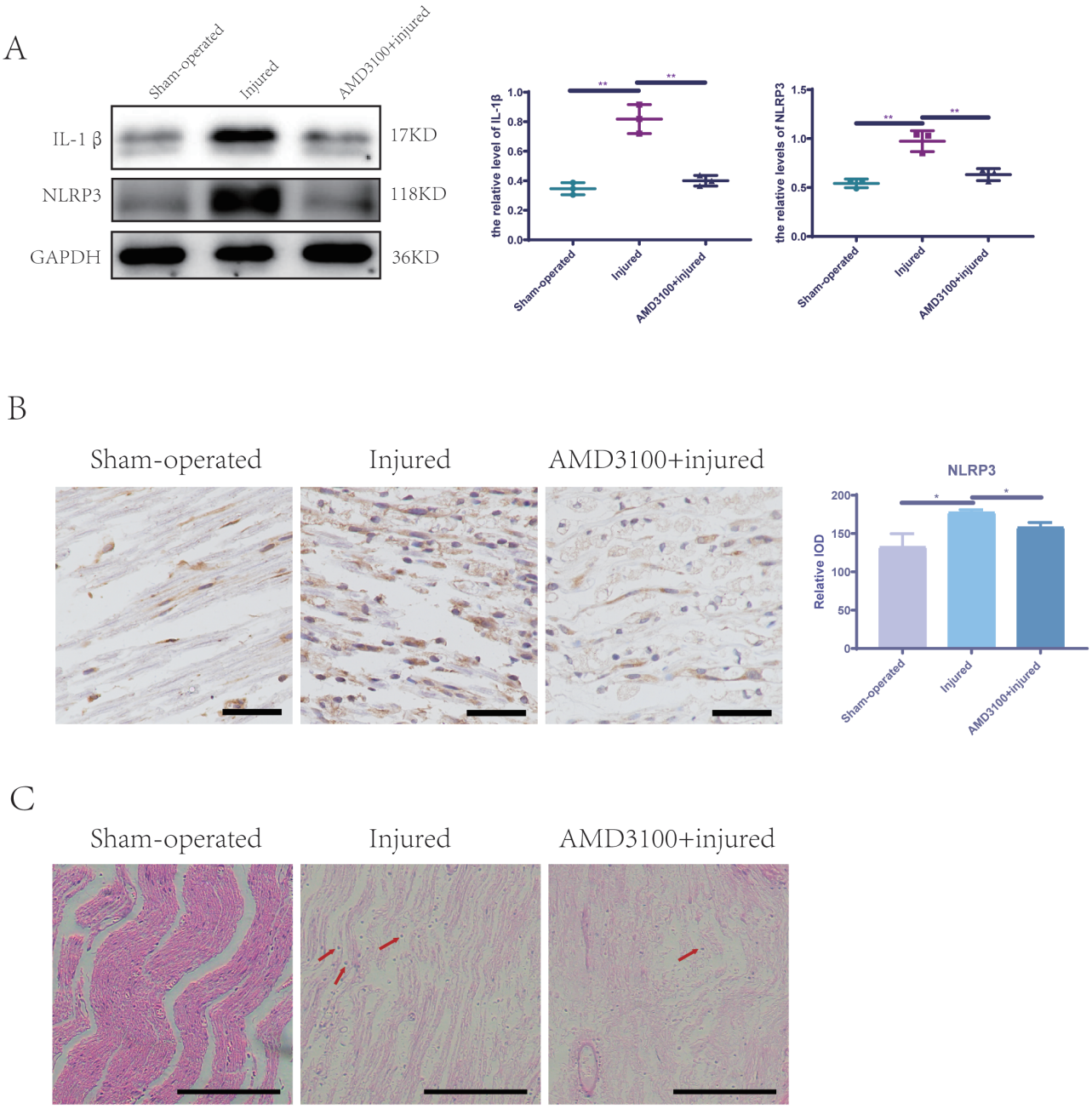

Figure 6. Intraperitoneal injection of AMD3100 alleviates the excessive inflammatory response in sciatic nerve after sciatic nerve injury. (A) The expression of IL-1β and NLRP3 in injured rats were markedly increased compared with the sham-operated rats 24 h after sciatic nerve injury, and AMD3100 (2.5 μg/ml) markedly reduced the protein levels of them. (B) Immunohistochemical staining of NLRP3 24 hours after sciatic nerve injury. The levels of NLRP3 were lower in AMD3100 pretreatment rats than that without AMD3100 pretreatment rats 24 h after sciatic nerve injury. Scale bars: 25 μm. (C) HE staining of the sciatic nerve of sham-operated rats, injured rats with or without AMD3100 treatment. Injured rats with AMD3100 pretreatment had lower inflammation than injured rats without AMD3100 pretreatment. Scale bars: 200 μm. Data are expressed as the mean ± SD of three independent experiments ($n = 9$ (A) and 9 (B, C)). $^{*}P < 0.05$, $^{**}P < 0.01$ (Student's t test).

of the LPS + ATP-treated group (Figure 8A). In addition, western blot analysis of extracted animal tissues also demonstrated that AMD3100 markedly reduced the expression of P-NF-κB and TXNIP in injured sciatic nerve (Figure 8B). Therefore, it can be concluded that CXCL12 and CXCR4 may promote the expression of NLRP3 by promoting NF-κB phosphorylation on the one hand, and the activation of NLRP3 inflammasome by promoting intracellular TXNIP expression on the other hand.

Discussion

In our study, both *in vitro* cellular inflammation models and *in vivo* sciatic nerve injury models demonstrated that the NLRP3 inflammasome was significantly activated in inflammatory Schwann cells. And the number of Schwann cells in the distal site of the sciatic nerve injury *in vivo* was lower than that of the sham-operated group and AMD3100 + injured group, which was consistent with the increased Schwann cell pyroptosis *in vitro*. Since Schwann cells are myelinating cells

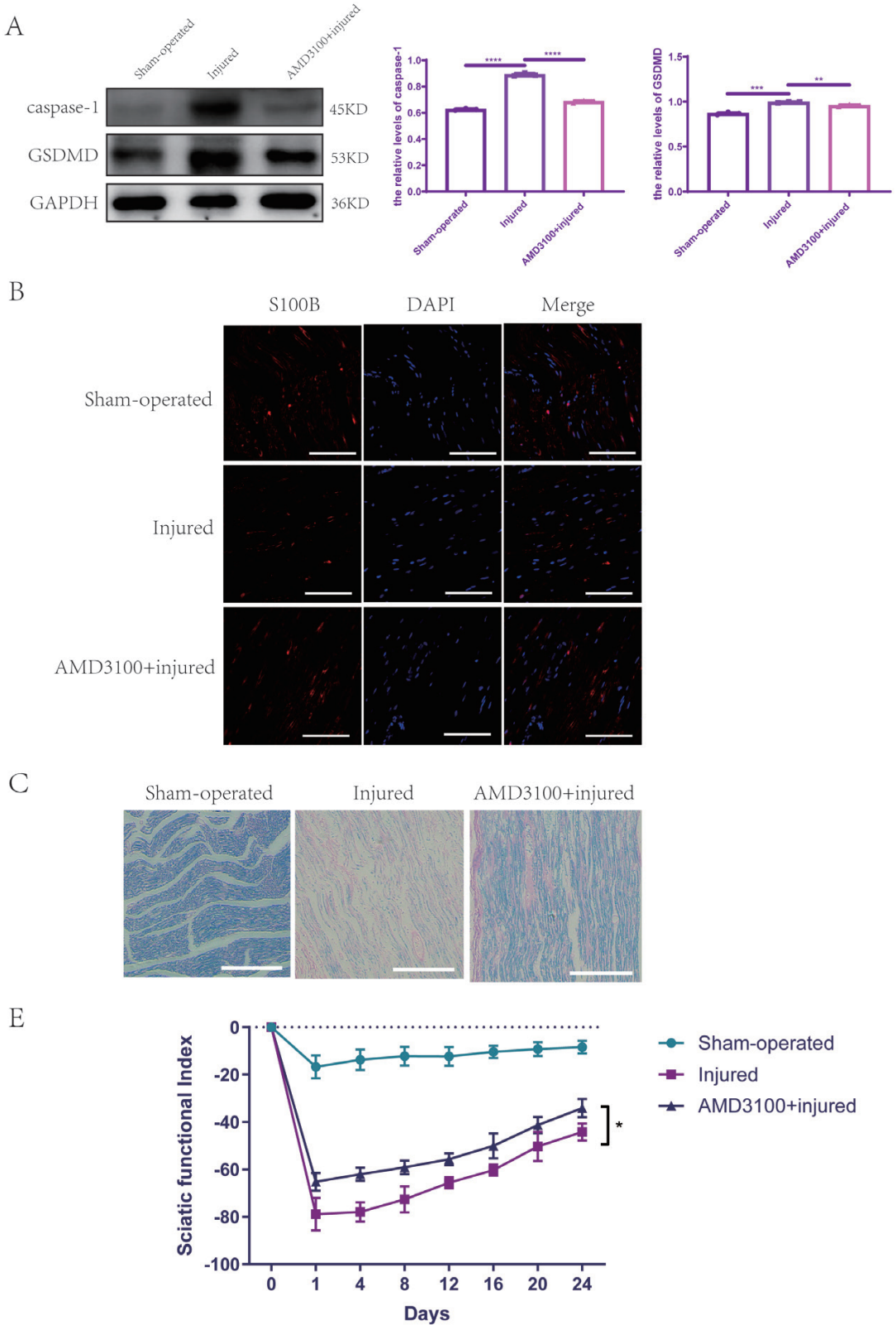

Figure 7. AMD3100 attenuates the pyroptosis and demyelination of Schwann cells in injured distal sciatic nerve. (A) AMD3100 attenuated the expression of pyroptosis-related proteins, GSDMD and caspase-1, in Schwann cells at the distal site of the injured sciatic nerve. (B) Immunofluorescence analysis of Schwann cells, labeled by S100B (Red, Cy3), in distal sites of sciatic nerve injury. The number of Schwann cells decreased in the injured group, and AMD3100 alleviated the reduction of Schwann cells caused by sciatic nerve injury in AMD3100+injured group. Scale bars: = 100 μm. (C) LFB staining of the sciatic nerve of sham-operated rats and injured rats with or without AMD3100. The demyelination was obvious in the injured group, and AMD3100 alleviated the demyelination caused by sciatic nerve injury in AMD3100+injured group. Scale bars: 200 μm. (D)The sciatic nerve function index (SFI). Data are the mean ± SD of three independent experiments (n = 9 (A), 9 (B, C) and 9 (D); *P < 0.05, **P < 0.01, ***P < 0.001, ****P < 0.0001 (Student's t test in (A, C) and two-way ANOVA in (D)).

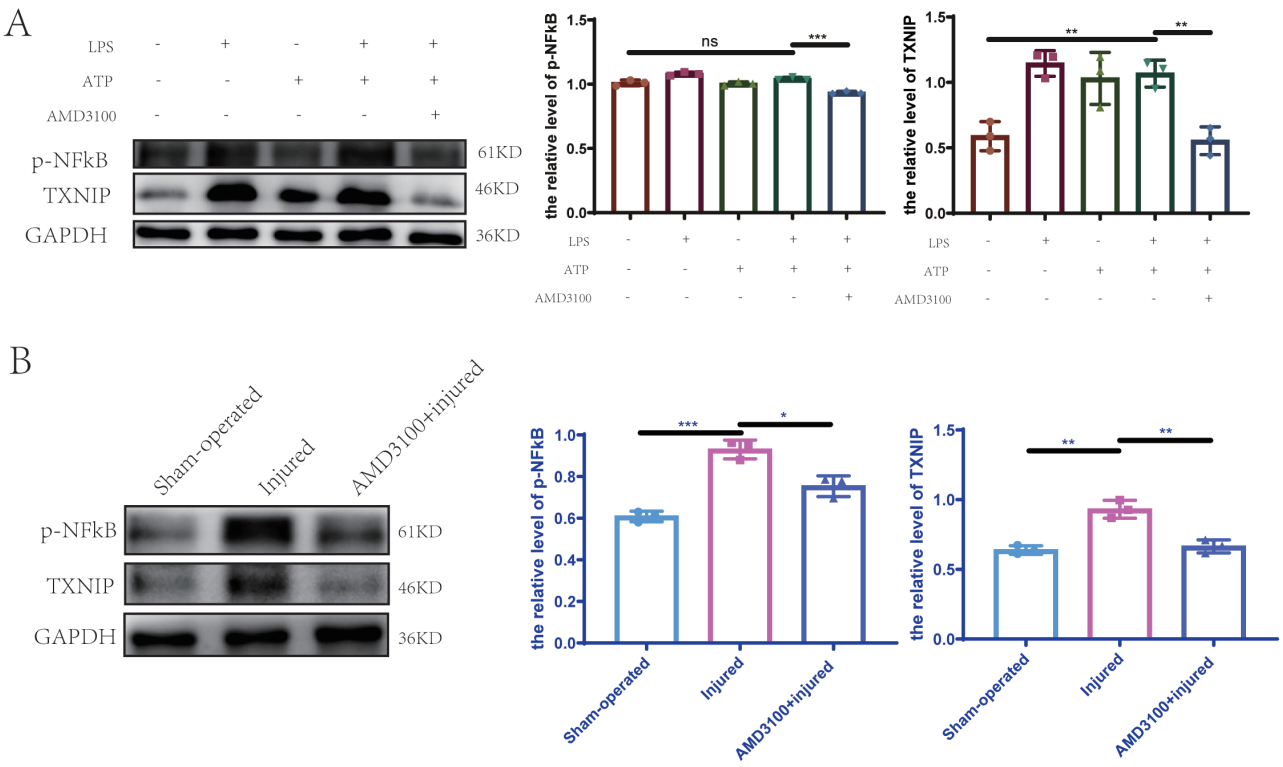

Figure 8. p-NF-κB and TXNIP may act as the downstream factors of CXCR4 to regulate the activation of NLRP3 inflammasome. (A) *In vitro* experiments, the increase in the expression of p-NF-κB and TXNIP in LPS + ATP group were decreased upon AMD3100 treatment. (B) *In vivo* animal experiments, both of p-NF-κB and TXNIP elevated in injured rats were also markedly decreased with AMD3100 treatment, which was consistent with the results of Schwann cells line. Data are expressed as the mean ± SD of three independent experiments ($n = 9$ (B)). $^{*}P < 0.05$, $^{**}P < 0.01$, $^{***}P < 0.001$ (Student's t test).

wrapped around axon fibers, we studied the demyelination of sciatic nerve and found that the demyelination of sciatic nerve was significant in the injured group, which corresponded to the increase in pyroptosis and the decrease in the number of Schwann cells in the injured group. Therefore, our results show that Schwann cells pyroptosis induced by the NLRP3 inflammasome leads to decreased Schwann cell numbers and demyelination after sciatic nerve injury.

In our study, we first confirmed the existence of CXCL12-CXCR4 autocrine pathway in RSC96 Schwann cells (Figure 3). The increased expression of CXCL12 and CXCR4 in Schwann cells are consistent with enhanced NLRP3 inflammasome activation, pyroptosis, inflammatory response, and sciatic nerve demyelination which was reversed by the effect of the AMD3100 inhibitor. In addition, the results of SFI also showed that AMD3100 can accelerate the recovery of nerve function to a certain extent, which may be due to the fact that AMD3100 can alleviate the demyelination of sciatic nerve caused by Schwann cell pyroptosis, and it may also block the role of CXCL12 from peripheral nerve injury and reduces the recruitment of circulating monocyte macrophages to the central nervous system and the production of IL-1β that aggravates nerve pain [65–67], thus alleviating neuropathic pain and favoring recovery of SFI. It has been early proved that CXCL12 interacts with active CXCR4 to promote the death of rat Schwann cells [68]. Moreover, it has been shown that Schwann cells can partially die after sciatic nerve compression injury [69], and there are more evidence that Schwann cells death or functional impairment under inflammatory conditions of diabetic peripheral nerve injury [70, 71]. Therefore, the partially death of Schwann cells in the early stage of sciatic nerve injury may be related to the acute inflammation response. However, few studies have proved how Schwann cells die after sciatic nerve injury. Our study has verified a way of Schwann cell death after sciatic nerve injury from the perspective of Schwann cell pyroptosis.

In addition, our study demonstrated that p-NF-κB and TXNIP expression was increased in Schwann cells and sciatic nerve of rats, which was consistent with the increased CXCR4 expression. AMD3100 decreased the protein levels of p-NF-κB and TXNIP, indicating that CXCL12-CXCR4 can promote the expression of p-NF-κB and TXNIP. Therefore, p-NF-κB may act as a signaling molecule downstream of CXCR4 to promote the expression of NLRP3 and pro-IL-1β, and TXNIP may affects the activation of NLRP3 inflammasome. However, due to previous studies have demonstrated that the p-NF-κB-NLRP3 and the TXNIP-NLRP3 inflammasome axis in the sciatic nerve are involved in the inflammation response and pain caused by sciatic nerve injury or lesion [34, 62, 72–75], we did not further verify the effect of p-NF-κB and TXNIP on the expression and activation of NLRP3 inflammasome by inhibiting them.

In summary, we have demonstrated the mechanism and role of the CXCL12-CXCR4 axis in peripheral nerve injury from the perspective of Schwann cell immune response. Our results showed that during the acute inflammatory response 24 h after sciatic nerve injury, large amounts of CXCL12 produced by Schwann cells was secreted extracellularly and could bind to CXCR4 on the cell membrane in an autocrine manner. And then CXCL12-CXCR4 can promote the activation of NLRP3

inflammasome and pyroptosis of Schwann cells possibly via p-NF-κB and TXNIP. The pyroptosis of Schwann cells promoted demyelination of the sciatic nerve, which might be not conducive to the recovery of sciatic nerve function.

Acknowledgements

The authors wish to thank the Natural Science Foundation of Shandong Province, China (grant number ZR2022MH029) and the Natural Science Foundation of Qingdao, Shandong (grant number 22-3-7-smjk-7-nsh).

Funding

This work was supported by the Natural Science Foundation of Shandong Province, China (grant number ZR2022MH029) and the Natural Science Foundation of Qingdao, Shandong (grant number 22-3-7-smjk-7-nsh).

Conflict of interests

The authors declare that they have no conflicts of interest.

Author contributions

Wei Li and Jie Liang contributed to the conception and design of the study. Wei Li contributed markedly to the literature search, experiment and data acquisition. Jie Liang performed the data analysis and statistical analysis. Shaohua Li, Meiying Song, Suli Jiang and Shuo Xu prepared the manuscript. Haining Meng, Dongchang Zhai and Lei Tang reviewed the manuscript. Luoyang Wang, Yanyan Yang, and Bei Zhang took responsibility for the integrity of the work as a whole from inception to published article.

Ethical approval

The animal research adheres to the ARRIVE guidelines (https://arriveguidelines.org/arrive-guidelines).

Data availability

The data that support the findings of this study are available on reasonable request from the corresponding author.

References

1. Wang J, Ou SW, Bai YF, Wang YJ, Xu ZD, Luan GM. Downregulation of adult and neonatal Nav1.5 in the dorsal root ganglia and axon of peripheral sensory neurons of rats with spared nerve injury. *Int J Mol Med* 2018, 41, 2225–32. doi:10.3892/ijmm.2018.3446.
2. Nascimento AI, Mar FM, Sousa MM. The intriguing nature of dorsal root ganglion neurons: Linking structure with polarity and function. *Prog Neurobiol* 2018, 168, 86–103. doi:10.1016/j.pneurobio.2018.05.002.
3. Bonanomi D. Axon pathfinding for locomotion. *Semin Cell Dev Biol* 2019, 85, 26–35. doi:10.1016/j.semcdb.2017.11.014.
4. Pei BA, Zi JH, Wu LS, Zhang CH, Chen YZ. Pulsed electrical stimulation protects neurons in the dorsal root and anterior horn of the spinal cord after peripheral nerve injury. *Neural Regener Res* 2015, 10, 1650–5. doi:10.4103/1673-5374.167765.
5. Jessen KR, Mirsky R. The repair Schwann cell and its function in regenerating nerves. *J Physiol* 2016, 594, 3521–31. doi:10.1113/JP270874.
6. Li W, Liang J, Li S, Wang L, Xu S, Jiang S, et al. Research progress of targeting NLRP3 inflammasome in peripheral nerve injury and pain. *Int Immunopharmacol* 2022, 110, 109026. doi:10.1016/j.intimp.2022.109026.
7. Freria CM, Bernardes D, Almeida GL, Simões GF, Barbosa GO, Oliveira AL. Impairment of toll-like receptors 2 and 4 leads to compensatory mechanisms after sciatic nerve axotomy. *J Neuroinflammation* 2016, 13, 118. doi:10.1186/s12974-016-0579-6.
8. Goethals S, Ydens E, Timmerman V, Janssens S. Toll-like receptor expression in the peripheral nerve. *Glia* 2010, 58, 1701–9. doi:10.1002/glia.21041.
9. Brosius Lutz A, Lucas TA, Carson GA, Caneda C, Zhou L, Barres BA, et al. An RNA-sequencing transcriptome of the rodent Schwann cell response to peripheral nerve injury. *J Neuroinflammation* 2022, 19, 105. doi:10.1186/s12974-022-02462-6.
10. Franchi L, Warner N, Viani K, Nuñez G. Function of Nod-like receptors in microbial recognition and host defense. *Immunol Rev* 2009, 227, 106–28. doi:10.1111/j.1600-065X.2008.00734.x.
11. Lamkanfi M, Dixit VM. Mechanisms and functions of inflammasomes. *Cell* 2014, 157, 1013–22. doi:10.1016/j.cell.2014.04.007.
12. Que YY, Zhu T, Zhang FX, Peng J. Neuroprotective effect of DUSP14 overexpression against isoflurane-induced inflammatory response, pyroptosis and cognitive impairment in aged rats through inhibiting the NLRP3 inflammasome. *Eur Rev Med Pharmacol Sci* 2020, 24, 7101–13. doi:10.26355/eurrev_202006_21704.
13. She Y, Shao L, Zhang Y, Hao Y, Cai Y, Cheng Z, et al. Neuroprotective effect of glycosides in Buyang Huanwu Decoction on pyroptosis following cerebral ischemia-reperfusion injury in rats. *J Ethnopharmacol* 2019, 242, 112051. doi:10.1016/j.jep.2019.112051.
14. Han X, Sun S, Sun Y, Song Q, Zhu J, Song N, et al. Small molecule-driven NLRP3 inflammation inhibition via interplay between ubiquitination and autophagy: implications for Parkinson disease. *Autophagy* 2019, 15, 1860–81. doi:10.1080/15548627.2019.1596481.
15. Holbrook JA, Jarosz-Griffiths HH, Caseley E, Lara-Reyna S, Poulter JA, Williams-Gray CH, et al. Neurodegenerative disease and the NLRP3 inflammasome. *Front Pharmacol* 2021, 12, 643254. doi:10.3389/fphar.2021.643254.
16. Chen Y, Meng J, Bi F, Li H, Chang C, Ji C, et al. EK7 regulates NLRP3 inflammasome activation and neuroinflammation post-traumatic brain injury. *Front Mol Neurosci* 2019, 12, 202. doi:10.3389/fnmol.2019.00202.
17. Han C, Yang Y, Guan Q, Zhang X, Shen H, Sheng Y, et al. New mechanism of nerve injury in Alzheimer's disease: β-amyloid-induced neuronal pyroptosis. *J Cell Mol Med* 2020, 24, 8078–90. doi:10.1111/jcmm.15439.
18. Cheng YC, Chu LW, Chen JY, Hsieh SL, Chang YC, Dai ZK, et al. Loganin attenuates high glucose-induced Schwann cells pyroptosis by inhibiting ROS generation and NLRP3 inflammasome activation. *Cells* 2020, 9, 1948. doi:10.3390/cells9091948.
19. Sagers JE, Sahin MI, Moon I, Ahmed SG, Stemmer-Rachamimov A, Brenner GJ, et al. NLRP3 inflammasome activation in human vestibular schwannoma: Implications for tumor-induced hearing loss. *Hear Res* 2019, 381, 107770. doi:10.1016/j.heares.2019.07.007.
20. Cui M, Liang J, Xu D, Zhao L, Zhang X, Zhang L, et al. NLRP3 inflammasome is involved in nerve recovery after sciatic nerve injury. *Int Immunopharmacol* 2020, 84, 106492. doi:10.1016/j.intimp.2020.106492.
21. Li M, Ransohoff RM. Multiple roles of chemokine CXCL12 in the central nervous system: a migration from immunology to neurobiology. *Prog Neurobiol* 2008, 84, 116–31. doi:10.1016/j.pneurobio.2007.11.003.
22. Küry P, Greiner-Petter R, Cornely C, Jürgens T, Müller HW. Mammalian achaete scute homolog 2 is expressed in the adult sciatic nerve and regulates the expression of Krox24, Mob-1, CXCR4, and p57kip2 in Schwann cells. *J Neurosci* 2002, 22, 7586–95. doi:10.1523/JNEUROSCI.22-17-07586.2002.

23. Gleichmann M, Gillen C, Czardybon M, Bosse F, Greiner-Petter R, Auer J, et al. Cloning and characterization of SDF-1gamma, a novel SDF-1 chemokine transcript with developmentally regulated expression in the nervous system. *Eur J Neurosci* 2000, 12, 1857–66. doi:10.1046/j.1460-9568.2000.00048.x.
24. Zanetti G, Negro S, Megighian A, Mattarei A, Lista F, Fillo S, et al. A CXCR4 receptor agonist strongly stimulates axonal regeneration after damage. *Ann Clin Transl Neurol* 2019, 6, 2395–402. doi:10.1002/acn3.50926.
25. Shi Y, Riese DJ 2nd, Shen J. The role of the CXCL12/CXCR4/CXCR7 chemokine axis in cancer. *Front Pharmacol* 2020, 11, 574667. doi:10.3389/fphar.2020.574667.
26. Negro S, Lessi F, Duregotti E, Aretini P, La Ferla M, Franceschi S, et al. Montecucco, CXCL12α/SDF-1 from perisynaptic Schwann cells promotes regeneration of injured motor axon terminals. *EMBO Mol Med* 2017, 9, 1000–10. doi:10.15252/emmm.201607257.
27. Gao D, Tang T, Zhu J, Tang Y, Sun H, Li S. CXCL12 has therapeutic value in facial nerve injury and promotes Schwann cells autophagy and migration via PI3K-AKT-mTOR signal pathway. *Int J Biol Macromol* 2019, 124, 460–8. doi:10.1016/j.ijbiomac.2018.10.212.
28. Han Y, He T, Huang DR, Pardo CA, Ransohoff RM. TNF-alpha mediates SDF-1 alpha-induced NF-kappa B activation and cytotoxic effects in primary astrocytes. *J Clin Invest* 2001, 108, 425–35. doi:10.1172/JCI12629.
29. Hou J, Wang C, Ma D, Chen Y, Jin H, An Y, et al. The cardioprotective and anxiolytic effects of Chaihujialonggumuli granule on rats with anxiety after acute myocardial infarction is partly mediated by suppression of CXCR4/NF-κB/GSDMD pathway. *Biomed Pharmacother* 2021, 133, 111015. doi:10.1016/j.biopha.2020.111015.
30. Wang YH, Tang YR, Gao X, Liu J, Zhang NN, Liang ZJ, et al. The anti-inflammatory and analgesic effects of intraperitoneal melatonin after spinal nerve ligation are mediated by inhibition of the NF-κB/NLRP3 inflammasome signaling pathway. *Brain Res Bull* 2021, 169, 156–66. doi:10.1016/j.brainresbull.2021.01.015.
31. Wang YH, Gao X, Tang YR, Yu Y, Sun MJ, Chen FQ, et al. The role of NF-κB/NLRP3 inflammasome signaling pathway in attenuating pyroptosis by melatonin upon spinal nerve ligation models. *Neurochem Res* 2022, 47, 335–46. doi:10.1007/s11064-021-03450-7.
32. He Y, Hara H, Núñez G. Mechanism and regulation of NLRP3 inflammasome activation. *Trends Biochem Sci* 2016, 41, 1012–21. doi:10.1016/j.tibs.2016.09.002.
33. Cheng KI, Chen SL, Hsu JH, Cheng YC, Chang YC, Lee CH, et al. Loganin prevents CXCL12/CXCR4-regulated neuropathic pain via the NLRP3 inflammasome axis in nerve-injured rats. *Phytomedicine* 2021, 92, 153734. doi:10.1016/j.phymed.2021.153734.
34. Pan Z, Shan Q, Gu P, Wang XM, Tai LW, Sun M, et al. miRNA-23a/CXCR4 regulates neuropathic pain via directly targeting TXNIP/NLRP3 inflammasome axis. *J Neuroinflammation* 2018, 15, 29. doi:10.1186/s12974-018-1073-0.
35. Mahmood DF, Abderrazak A, El Hadri K, Simmet T, Rouis M. The thioredoxin system as a therapeutic target in human health and disease. *Antioxid Redox Signal* 2013, 19, 1266–303. doi:10.1089/ars.2012.4757.
36. Du RH, Wu FF, Lu M, Shu XD, Ding JH, Wu G, et al. Uncoupling protein 2 modulation of the NLRP3 inflammasome in astrocytes and its implications in depression. *Redox Biol* 2016, 9, 178–87. doi:10.1016/j.redox.2016.08.006.
37. Wang CY, Xu Y, Wang X, Guo C, Wang T, Wang ZY. Dl-3-n-Butylphthalide Inhibits NLRP3 Inflammasome and Mitigates Alzheimer's-Like Pathology via Nrf2-TXNIP-TrX Axis. *Antioxid Redox Signal* 2019, 30, 1411–31. doi:10.1089/ars.2017.7440.
38. Xu W, Li T, Gao L, Zheng J, Yan J, Zhang J, et al. Apelin-13/APJ system attenuates early brain injury via suppression of endoplasmic reticulum stress-associated TXNIP/NLRP3 inflammasome activation and oxidative stress in a AMPK-dependent manner after subarachnoid hemorrhage in rats. *J Neuroinflammation* 2019, 16, 247. doi:10.1186/s12974-019-1620-3.
39. Wang M, Liu Z, Hu S, Duan X, Zhang Y, Peng C, et al. Taohong siwu decoction ameliorates ischemic stroke injury via suppressing pyroptosis. *Front Pharmacol* 2020, 11, 590453. doi:10.3389/fphar.2020.590453.
40. Al Mamun A, Wu Y, Monalisa I, Jia C, Zhou K, Munir F, et al. Role of pyroptosis in spinal cord injury and its therapeutic implications. *J Adv Res* 2021, 28, 97–109. doi:10.1016/j.jare.2020.08.004.
41. Hou Y, Wang Y, He Q, Li L, Xie H, Zhao Y, et al. Nrf2 inhibits NLRP3 inflammasome activation through regulating Trx1/TXNIP complex in cerebral ischemia reperfusion injury. *Behav Brain Res* 2018, 336, 32–9. doi:10.1016/j.bbr.2017.06.027.
42. Zhou Y, Chen Z, Yang X, Cao X, Liang Z, Ma H, et al. Morin attenuates pyroptosis of nucleus pulposus cells and ameliorates intervertebral disc degeneration via inhibition of the TXNIP/NLRP3/Caspase-1/IL-1β signaling pathway. *Biochem Biophys Res Commun* 2021, 559, 106–12. doi:10.1016/j.bbrc.2021.04.090.
43. Han Y, Xu X, Tang C, Gao P, Chen X, Xiong X, et al. Reactive oxygen species promote tubular injury in diabetic nephropathy: The role of the mitochondrial ros-txnip-nlrp3 biological axis. *Redox Biol* 2018, 16, 32–46. doi:10.1016/j.redox.2018.02.013.
44. Boivin A, Pineau I, Barrette B, Filali M, Vallières N, Rivest S, et al. Toll-like receptor signaling is critical for Wallerian degeneration and functional recovery after peripheral nerve injury. *J Neurosci* 2007, 27, 12565–76. doi:10.1523/JNEUROSCI.3027-07.2007.
45. Percie du Sert N, Hurst V, Ahluwalia A, Alam S, Avey MT, Baker M, et al. The ARRIVE guidelines 2.0: Updated guidelines for reporting animal research. *PLoS Biol* 2020, 18, e3000410. doi:10.1371/journal.pbio.3000410.
46. Percie du Sert N, Ahluwalia A, Alam S, Avey MT, Baker M, Browne WJ, et al. Reporting animal research: explanation and elaboration for the ARRIVE guidelines 2.0. *PLoS Biol* 2020, 18, e3000411. doi:10.1371/journal.pbio.3000411.
47. Xu D, Liang J, Cui M, Zhang L, Ren S, Zheng W, et al. Saturated fatty acids activate the inflammatory signalling pathway in Schwann cells: implication in sciatic nerve injury. *Scand J Immunol* 2020, 92, e12896. doi:10.1111/sji.12896.
48. Livak KJ, Schmittgen TD. Analysis of relative gene expression data using real-time quantitative PCR and the 2(-Delta Delta C(T)) Method. *Methods (San Diego, Calif.)* 2001, 25, 402–8. doi:10.1006/meth.2001.1262.
49. Dunbar A, Schauwvlieghe A, Algoe S, van Hellemond JJ, Reynders M, Vandecasteele S, et al. Epidemiology of *Pneumocystis jirovecii* Pneumonia and (Non-)use of prophylaxis. *Front Cell Infect Microbiol* 2020, 10, 224. doi:10.3389/fcimb.2020.00224.
50. Varejão AS, Meek MF, Ferreira AJ, Patrício JA, Cabrita AM. Functional evaluation of peripheral nerve regeneration in the rat: walking track analysis. *J Neurosci Methods* 2001, 108, 1–9. doi:10.1016/s0165-0270(01)00378-8.
51. Baptista AF, Gomes JR, Oliveira JT, Santos SM, Vannier-Santos MA, Martinez AM. A new approach to assess function after sciatic nerve lesion in the mouse - adaptation of the sciatic static index. *J Neurosci Methods* 2007, 161, 259–64. doi:10.1016/j.jneumeth.2006.11.016.
52. Geuna S. The sciatic nerve injury model in pre-clinical research. *J Neurosci Methods* 2015, 243, 39–46. doi:10.1016/j.jneumeth.2015.01.021.
53. Wang J, Tannous BA, Poznansky MC, Chen H. CXCR4 antagonist AMD3100 (plerixafor): From an impurity to a therapeutic agent. *Pharmacol Res* 2020, 159, 105010. doi:10.1016/j.phrs.2020.105010.
54. Huang Y, Xu W, Zhou R. NLRP3 inflammasome activation and cell death. *Cell Mol Immunol* 2021, 18, 2114–27. doi:10.1038/s41423-021-00740-6.
55. Bucan V, Vaslaitis D, Peck CT, Strauß S, Vogt PM, Radtke C. Effect of exosomes from rat adipose-derived mesenchymal stem cells on neurite outgrowth and sciatic nerve regeneration after crush injury. *Mol Neurobiol* 2019, 56, 1812–24. doi:10.1007/s12035-018-1172-z.
56. Ma Z, Zhou Y, Wang Y, Xu Y, Liu Y, Liu Y, et al. RNA-binding protein hnRNP UL1 binds κB sites to attenuate NF-κB-mediated

inflammation. *J Autoimmun* 2022, 129, 102828. doi:10.1016/j.jaut.2022.102828.
57. Harpio R, R, Einarsson., S100 proteins as cancer biomarkers with focus on S100B in malignant melanoma. *Clin Biochem* 2004, 37, 512–8. doi:10.1016/j.clinbiochem.2004.05.012.
58. Abdo H, Calvo-Enrique L, Lopez JM, Song J, Zhang MD, Usoskin D, et al. Specialized cutaneous Schwann cells initiate pain sensation. *Science (New York, N.Y.)* 2019, 365, 695–9. doi:10.1126/science.aax6452.
59. Sun R, Peng M, Xu P, Huang F, Xie Y, Li J, et al. Low-density lipoprotein receptor (LDLR) regulates NLRP3-mediated neuronal pyroptosis following cerebral ischemia/reperfusion injury. *J Neuroinflammation* 2020, 17, 330. doi:10.1186/s12974-020-01988-x.
60. Liang Y, Song P, Chen W, Xie X, Luo R, Su J, et al. Inhibition of caspase-1 ameliorates ischemia-associated blood-brain barrier dysfunction and integrity by suppressing pyroptosis activation. *Front Cell Neurosci* 2020, 14, 540669. doi:10.3389/fncel.2020.540669.
61. Park S, Jung N, Myung S, Choi Y, Chung KW, Choi BO, et al. Differentiation of human tonsil-derived mesenchymal stem cells into Schwann-like cells improves neuromuscular function in a mouse model of charcot-marie-tooth disease type 1A. *Int J Mol Sci* 2018, 19, 2393. doi:10.3390/ijms19082393.
62. Miao J, Zhou X, Ji T, Chen G. NF-κB p65-dependent transcriptional regulation of histone deacetylase 2 contributes to the chronic constriction injury-induced neuropathic pain via the microRNA-183/TXNIP/NLRP3 axis. *J Neuroinflammation* 2020, 17, 225. doi:10.1186/s12974-020-01901-6.
63. Kelley N, Jeltema D, Duan Y, He Y. The NLRP3 inflammasome: an overview of mechanisms of activation and regulation. *Int J Mol Sci* 2019, 20, 3328. doi:10.3390/ijms20133328.
64. Liu Y, Zhang Z, Li W, Tian S. PECAM1 combines with CXCR4 to trigger inflammatory cell infiltration and pulpitis progression through activating the NF-κB signaling pathway. *Front Cell Dev Biol* 2020, 8, 593653. doi:10.3389/fcell.2020.593653.
65. Mai CL, Tan Z, Xu YN, Zhang JJ, Huang ZH, Wang D, et al. CXCL12-mediated monocyte transmigration into brain perivascular space leads to neuroinflammation and memory deficit in neuropathic pain. *Theranostics* 2021, 11, 1059–78. doi:10.7150/thno.44364.
66. Wolf G, Gabay E, Tal M, Yirmiya R, Shavit Y. Genetic impairment of interleukin-1 signaling attenuates neuropathic pain, autotomy, and spontaneous ectopic neuronal activity, following nerve injury in mice. *Pain* 2006, 120, 315–24. doi:10.1016/j.pain.2005.11.011.
67. Guo YJ, Li HN, Ding CP, Han SP, Wang JY. Red nucleus interleukin-1β evokes tactile allodynia through activation of JAK/STAT3 and JNK signaling pathways. *J Neurosci Res* 2018, 96, 1847–61. doi:10.1002/jnr.24324.
68. Küry P, Köller H, Hamacher M, Cornely C, Hasse B, Müller HW. Cyclic AMP and tumor necrosis factor-alpha regulate CXCR4 gene expression in Schwann cells. *Mol Cell Neurosci* 2003, 24, 1–9. doi:10.1016/s1044-7431(03)00132-5.
69. Govindappa PK, Elfar JC. Erythropoietin promotes M2 macrophage phagocytosis of Schwann cells in peripheral nerve injury. *Cell Death Dis* 2022, 13, 245. doi:10.1038/s41419-022-04671-6.
70. Kornelius E, Tsou SH, Chang CC, Ho YJ, Lin SC, Chen WL, et al. Liraglutide attenuates glucolipotoxicity-induced RSC96 Schwann cells' inflammation and dysfunction. *Biomolecules* 2022, 12, 1338. doi:10.3390/biom12101338.
71. Zhang X, Zhao S, Yuan Q, Zhu L, Li F, Wang H, et al. TXNIP, a novel key factor to cause Schwann cell dysfunction in diabetic peripheral neuropathy, under the regulation of PI3K/Akt pathway inhibition-induced DNMT1 and DNMT3a overexpression. *Cell Death Dis* 2021, 12, 642. doi:10.1038/s41419-021-03930-2.
72. Liu P, Cheng J, Ma S, Zhou J. Paeoniflorin attenuates chronic constriction injury-induced neuropathic pain by suppressing spinal NLRP3 inflammasome activation. *Inflammopharmacology* 2020, 28, 1495–508. doi:10.1007/s10787-020-00737-z.
73. Li C, Li X, Shi Z, Wu P, Fu J, Tang J, et al. Exosomes from LPS-preconditioned bone marrow MSCs accelerated peripheral nerve regeneration via M2 macrophage polarization: Involvement of TSG-6/NF-κB/NLRP3 signaling pathway. *Exp Neurol* 2022, 356, 114139. doi:10.1016/j.expneurol.2022.114139.
74. Derangula K, Javalgekar M, Kumar Arruri V, Gundu C, Kumar Kalvala A, Kumar A. Probucol attenuates NF-κB/NLRP3 signalling and augments Nrf-2 mediated antioxidant defence in nerve injury induced neuropathic pain. *Int Immunopharmacol* 2022, 102, 108397. doi:10.1016/j.intimp.2021.108397.
75. Han L, Xi G, Guo N, Guo J, Rong Q. Expression and mechanism of TXNIP/NLRP3 inflammasome in sciatic nerve of type 2 diabetic rats. *Dis Markers* 2022, 2022, 9696303. doi:10.1155/2022/9696303.